REDUCED-REFERENCE QUALITY METRIC FOR SCREEN CONTENT IMAGE

Zhaohui Che[†], *Guangtao Zhai*[†], *Ke Gu*[‡], *and Patrick Le Callet*[§]

[†]Insti. of Image Commu. and Infor. Proce., Shanghai Jiao Tong University, China
[‡]School of Computer Science and Engineering, Nanyang Technological University, Singapore
[§]Luman Université, Université de Nantes, IRCCyN UMR CNRS 6597, Polytech Nantes, France
Email: chezhaohui@sjtu.edu.cn

ABSTRACT

With the prevalence of digital products like cellphone, tablet and personal computer, the screen content image (SCI) consisting of text, graphic, and natural scene picture becomes a significant media in various communication scenarios. Consequently, we proposed a reduced-reference quality metric dedicated for SCI. The main contribution includes 2 aspects : **1)** we innovatively proposed a layer-based segmentation method to divide SCI into text layer and pictorial layer; **2)** we designed respective quality metrics dedicated for text and pictorial layers with a novel pooling strategy considering human visual saliency for SCI. Furthermore, exhaustive experimental results indicate that the proposed metric is highly comparative compared with state-of-the-art full-reference quality metrics.

Index Terms— Screen content, IQA, free energy

1. INTRODUCTION

Recently, screen content image (SCI) plays a critical role in diverse scenarios such as remote conferencing [1], screen capture, cloud transformation [2], etc. Moreover, with the prevalence of digital devices like cellphone and tablet, the ubiquitous SCIs occupy a large space of our mobile phone albums. However, most consumer-type SCIs are captured by amateurish devices which corrupt the SCIs with various distortions. Therefore, the quality of SCI is one of the most attractive issues for consumers and researchers.

A plenty of image quality assessment (IQA) metrics have been proposed in the past decades. However, most IQA metrics are designed for natural images which have significant differences with SCIs. Considering the complex components of SCIs, i.e. text area, graphic area, and natural scene picture area, the traditional IQA metrics fail to evaluate these informative compound images. Notably, a few new quality metrics dedicated for SCIs were proposed in recent years. Specifically, Yang *et al*. proposed a full-reference quality metric SPQA [3] in 2015. The SPQA developed the classic SSIM metric [4], and used it to estimate the text regions and pictorial regions separately. Whereas the SPQA fails to estimate distorted SCIs' quality unless obtaining complete information of the reference SCI. However, in practical situation, attaining and transmitting the complete reference SCI are costly, even impossible. Wang *et al*. came up with another full-reference SCI quality metric Q_s [5] based on SSIM. Although Q_s segmented SCI into text blocks and pictorial blocks, it destroys the integrity of natural scene pictures located at the SCI. Gu *et al*. proposed a full-reference structure-induced quality metric SIQM [6] in 2016. However, SIQM ignores the impacts of relationship between text and pictorial regions and distribution of pictorial regions in the SCI.

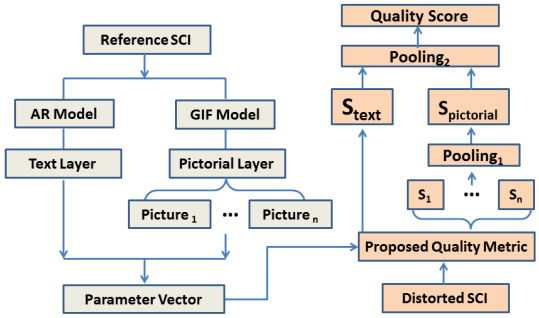

(a)

Fig. 1. Flowchart of the proposed quality metric.

Considering the drawbacks and flaws of the existing SCI quality metrics, we proposed a reduced-reference SCI quality assessment metric in this paper. The main contribution is divided into two aspects. Firstly, we proposed a novel layer-based segmentation algorithm to divide SCI into text and pictorial layers, so as to extract the accurate location, size and inclination angle of each picture located at the same SCI. Secondly, we designed two different reduced-reference quality metrics dedicated for pictorial and text layers. Specifically, incorporating with prior information of human visual saliency when viewing SCI, we proposed a novel pooling strategy and obtained the ultimate quality score of the SCI.

The rest of this paper is organized as follows. In section 2, we elaborated the proposed segmentation algorithm and quality metric in detail. The exhaustive experimental results were exhibited in section 3 for validating performance. We drew conclusions and gave out future directions in section 4.

2. REDUCED-REFERENCE QUALITY ASSESSMENT METRIC FOR SCREEN CONTENT IMAGE

2.1. Layer-based Segmentation Method

Above all, SCIs usually contain text areas and pictorial areas. In addition, most SCIs always contain several natural scene pictures scattered at arbitrary positions. Notably, text areas contain thin edges and small base colour numbers, while pictorial areas have thick boundaries and abundant colour. Accordingly, human visual perceptions of text and pictorial areas depend on different features. Driven by designing appropriative quality measurements for different areas while keeping the integrity of each picture located at the same SCI, we innovatively proposed a layer-based segmentation method.

The SCI segmentation methods have been investigated in recent years [8-11]. However, block-based methods [8,9] destroy the integrity of pictures, while layer-based methods [10,11] are not able to differentiate textual details of pictorial and text areas. Herein, in the proposed method, we divided a complete SCI into five layers, i.e. smooth background layer (SBL), smooth pictorial layer (SPL), textural pictorial layer (TPL), smooth text layer (STL), and textural text layer (TTL). Subsequently, we adopted spatial filtering techniques to extract TPL, TTL and SBL as follows.

Considering the heuristic information that text layer contains many short steep edges while pictorial layer contains chaotic texture details and thick boundaries, we adopted the autoregressive (AR) model [12] and guided image filter (GIF) [13] to process the SCI respectively, because the AR model has good texture-preserving ability while the GIF is good at preserving edges. The AR model specifies that the output depends linearly on its own previous variable value and on a stochastic term. In digital image processing, this relationship can be expressed by equation 1.

$$y_i = \boldsymbol{\alpha} \times \boldsymbol{\gamma}^k(y_i) + \varepsilon_i \tag{1}$$

where y_i is the pixel value to be processed; $\boldsymbol{\alpha} = \{\alpha_1, ..., \alpha_k\}$ is the vector of AR coefficients; $\boldsymbol{\gamma}^k(y_i)$ means the k member neighborhood vector of y_i; ε_i is the difference between ground truth and predicted value. The parameter $\boldsymbol{\alpha}$ can be solved via the linear system:

$$\hat{\boldsymbol{\alpha}} = \arg\min_{\boldsymbol{\alpha}} ||\boldsymbol{y} - \boldsymbol{Y}\boldsymbol{\alpha}||_2 \tag{2}$$

where $\boldsymbol{Y}(\boldsymbol{i},:) = \boldsymbol{\gamma}^k(y_i)$ and $\boldsymbol{y} = (y_1, y_2, ..., y_k)$. We can solve this linear system by least square method and obtain the approximate solution as $\hat{\boldsymbol{\alpha}} = \left(\boldsymbol{Y^T Y}\right)^{-1}\boldsymbol{Y^Y y}$. The AR model can protect pictorial details well, but it performs poorly on steep edges of text. On the other hand, the GIF can generate output according to the guide image. GIF behaves as an efficient edge-preserving smoothing operator when the guide image is identical to the original input image.

After obtaining AR model filtering result I_{ar} and GIF filtering result I_{gif}, we calculated the coarse $\overline{TTL}$ and $\overline{TPL}$ by equation 3.

$$\begin{cases} \overline{\boldsymbol{TTL}} = 1 - \boldsymbol{N}(\text{SSIM}(\boldsymbol{I_{ar}}, \boldsymbol{I_{input}})) \\ \overline{\boldsymbol{TPL}} = 1 - \boldsymbol{N}(\text{SSIM}(\boldsymbol{I_{gif}}, \boldsymbol{I_{input}})) \end{cases} \tag{3}$$

For SSIM($\boldsymbol{I_{ar}}, \boldsymbol{I_{input}}$), the higher values mean that I_{ar} has the similar values with the original image I_{input} in the corresponding positions. Videlicet, the lower values represent the pixels with severe distortions, $i.e.$ coarse textural text layer $\overline{TTL}$. Therefore, the $\overline{TTL}$ can be obtained by equation 3, where $\boldsymbol{N}$ is a normalization function to make sure that the SSIM($\boldsymbol{I_{ar}}, \boldsymbol{I_{input}}$) is from 0 to 1. Analogously, we obtained the $\overline{TPL}$. It's worth noting that $\overline{TTL}$ also contains some sharp pictorial textural details which are similar to steep edges of text region, and vise versa. For refining coarse $\overline{TTL}$, we emphasized $\overline{TTL}$, while suppressed $\overline{TPL}$ by equation 4, and the same applies to $\overline{TPL}$.

$$\begin{cases} \boldsymbol{TTL} = \text{binary}(\max(\overline{\boldsymbol{TTL}} - \boldsymbol{w} \times \overline{\boldsymbol{TPL}}, \boldsymbol{0})) \\ \boldsymbol{TPL} = \text{binary}(\max(\overline{\boldsymbol{TPL}} - \boldsymbol{w} \times \overline{\boldsymbol{TTL}}, \boldsymbol{0})) \end{cases} \tag{4}$$

where weighting coefficient $\boldsymbol{w}$ is set equal to 2 based on a lot of experimental data. In addition, experimental data shows that most common SCIs, such as webpages and slides, have smooth backgrounds in a few base colors. Therefore, we found out the most frequent base colors accounting for at least 20% of all pixels, so that we could extract SBL in base colors. Heretofore, we obtained TTL, TPL, and SBL. However, remaining SPL and STL are difficult to differentiate since they have similar small variances. Consequently, we extracted a binary index map made up of SPL, TPL, and STL by $1 - SBL - TTL$ which is shown in Fig.2 (c).

2.2. Quality Metric for Pictorial Layer

Driven by saving transmitting cost, we refined a feature vector $\boldsymbol{V_r}$ from reference SCI as the reduced-reference information, rather than utilize every pixel of the reference SCI like [3-6]. Taking a departure from the binary index map as Fig.2 (c), we adopted Matlab function $bwareaopen.m$ to eliminate tiny STL of the index map, then extracted information of remaining connected regions by function $bwconncomp.m$. Specifically, the information includes the number $\boldsymbol{N_r}$ of connected regions (i.e. the number of natural scene pictures located at the reference SCI), and corresponding location information. Furthermore, for each picture I_i (i=1,$\cdots$,$\boldsymbol{N_r}$), we extracted the coordinate values [$X_{i,u}$, $Y_{i,u}$], [$X_{i,b}$, $Y_{i,b}$],[$X_{i,l}$, $Y_{i,l}$] and [$X_{i,r}$, $Y_{i,r}$] representing upper, bottom, left, and right corners of I_i respectively. Consequently, we easily calculated width $\boldsymbol{W_i}$ and height $\boldsymbol{H_i}$ of I_i. Notably, regardless of picture content, we defined the inclination angle $\boldsymbol{A_i}$ of I_i as equation 5.

$$\boldsymbol{A_i} = \arctan\left(\frac{|\boldsymbol{Y_{i,u}} - \boldsymbol{Y_{i,l}}|}{|\boldsymbol{X_{i,u}} - \boldsymbol{X_{i,l}}|}\right) \tag{5}$$

Furthermore, for picture I_i, we adopted FEDM metric [14] to calculate corresponding quality score $\boldsymbol{FE_{i,r}}$ based on free

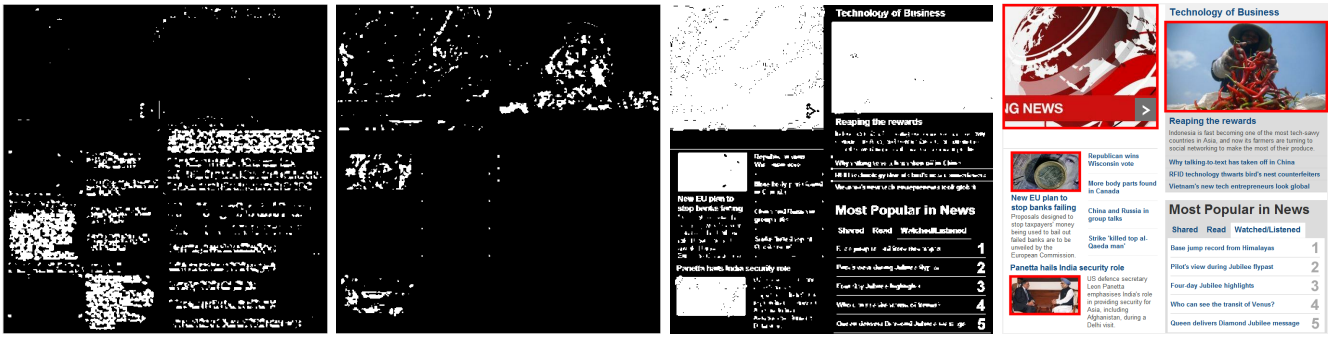

(a) (b) (c) (d)

Fig. 2. (a) Textural text layer (TTL). (b) Textural pictorial layer (TPL). (c) The index map including textural pictorial layer (TPL), smooth pictorial layer (SPL) and smooth text layer (STL). (d) Segmentation result.

energy principle. Concretely speaking, suppose that the internal generative model $\boldsymbol{g}$ of human brain is parametric for visual perception, and the perceived scene can be explained by adjusting the parameter vector $\boldsymbol{\phi}$. Given the input visual signal $\boldsymbol{s}$, its surprise (measured by entropy) can be attained by integrating the joint distribution $\boldsymbol{p(s,\phi|g)}$ over the space of model parameter $\boldsymbol{\phi}$. The free energy is defined as equation 6.

$$\boldsymbol{f(\phi)} = -\int \boldsymbol{q(\phi|s)} \log \frac{\boldsymbol{p(s,\phi)}}{\boldsymbol{q(\phi|s)}} \mathrm{d}\boldsymbol{\phi} \tag{6}$$

Considering the computational and operational aspects of free energy, we adopted AR model to simulate human brain generative model $\boldsymbol{g}$, so that the quantitative measurement of FEDM is defined as entropy of error map $I_{i,\Delta}$ between input image I_i and its AR model filtering result $I_{i,ar}$ ($I_{i,\Delta} = I_i - I_{i,ar}$).

$$\boldsymbol{FE_{i,r}} = -\sum_{k} \boldsymbol{p_k(I_{i,\Delta})} \log \boldsymbol{p_k(I_{i,\Delta})} \tag{7}$$

Heretofore, we obtained the parameter vector $\boldsymbol{V_r}$ as

$$\begin{cases} \boldsymbol{V_r} = \{\boldsymbol{V_{i,r}} | \boldsymbol{i} \in \{1, 2, \cdots, \boldsymbol{N_r}\}\} \\ \boldsymbol{V_{i,r}} = [\boldsymbol{X_{i,u}}, \boldsymbol{Y_{i,u}}, \boldsymbol{W_i}, \boldsymbol{H_i}, \boldsymbol{A_i}, \boldsymbol{FE_{i,r}}] \end{cases} \tag{8}$$

As suggested by research about webpage saliency [7], i.e. human visual fixations usually fall in the top-left region when viewing the SCIs, we proposed the top-left bias pooling strategy to emphasis the impact of pictures' locations on ultimate quality score $\boldsymbol{score_p}$ of pictorial layer.

$$\begin{cases} \boldsymbol{score_p} = \sum_{i=1}^{N_r} \boldsymbol{\mu_i} |\boldsymbol{FE_{i,r}} - \boldsymbol{FE_{i,d}}| \\ \boldsymbol{\mu_i} = \frac{\boldsymbol{D([X_{i,c}, Y_{i,c}], [1,1])^{-1}}}{\sum_{j=1}^{N_r} \boldsymbol{D([X_{j,c}, Y_{j,c}], [1,1])^{-1}}} \end{cases} \tag{9}$$

Where $\boldsymbol{FE_{i,d}}$ is the free energy quality index of the $\boldsymbol{i}$th picture $I_{i,d}$ located at the distorted SCI (we can easily find out the location of $I_{i,d}$ using $\boldsymbol{V_r}$). Specifically, the physical meaning of pooling coefficient $\boldsymbol{\mu_i}$ is the Euclidean distance (represented by $\boldsymbol{D}$) between centroid point $[\boldsymbol{X_{i,c}}, \boldsymbol{Y_{i,c}}]$ of picture $I_{i,d}$ and top-left corner $[\boldsymbol{1}, \boldsymbol{1}]$ of the distorted SCI. The centroid point $[\boldsymbol{X_{i,c}}, \boldsymbol{Y_{i,c}}]$ can be calculated as follows.

$$\begin{cases} \boldsymbol{X_{i,c}} = \boldsymbol{X_{i,u}} + \sqrt{(\frac{\boldsymbol{W_i}}{\boldsymbol{2}})^{\boldsymbol{2}} + (\frac{\boldsymbol{H_i}}{\boldsymbol{2}})^{\boldsymbol{2}}} \sin(\boldsymbol{A_i} + \arctan(\frac{\boldsymbol{H_i}}{\boldsymbol{W_i}})) \\ \boldsymbol{Y_{i,c}} = \boldsymbol{Y_{i,u}} + \sqrt{(\frac{\boldsymbol{W_i}}{\boldsymbol{2}})^{\boldsymbol{2}} + (\frac{\boldsymbol{H_i}}{\boldsymbol{2}})^{\boldsymbol{2}}} \cos(\boldsymbol{A_i} + \arctan(\frac{\boldsymbol{H_i}}{\boldsymbol{W_i}})) \end{cases} \tag{10}$$

2.3. Quality Metric for Text Layer

Experimental analysis about subjective scores of SCI database [3] pointed out that blur and contrast change were dominative distortions for text layer, because these distortion types impacted human perception severely when reading text. Therefore, in this section, we proposed two novel quality features for measuring contrast change and blurness of text layer.

Based on the parameters of $\boldsymbol{V_r}$ obtained in section 2.2, for each distorted SCI, we can easily extract a index map $\boldsymbol{M_t}$ made up of SBL, STL, and TTL. Subsequently, for $\boldsymbol{M_t}$, we found out the gray values of background and text by counting the frequence of each gray value. In other word, high quality text layer usually contains pure background and uniform text color, so that background and text gray values have largest frequences. Hence, the first feature is defined as

$$\boldsymbol{f_1} = \frac{1}{255} \frac{|\boldsymbol{B_r} - \boldsymbol{B_d}|}{|\boldsymbol{T_d} - \boldsymbol{B_d}| + C1} \tag{11}$$

where $\boldsymbol{B_r}$, $\boldsymbol{B_d}$ and $\boldsymbol{T_d}$ represent the gray values of reference SCI's background, distorted SCI's background and distorted SCI's text separately. C_1 is a positive constant (set as 1) used to avoid instability when denominator is close to zero. The weighting coefficient $\frac{1}{255}$ guarantees that the $\boldsymbol{f_1}$ is from 0 to 1. Obviously, higher $|\boldsymbol{B_r} - \boldsymbol{B_d}|$ means severe contrast change distortion, while lower $|\boldsymbol{T_d} - \boldsymbol{B_d}|$ means that the text and background of distorted SCI is in low contrast. Higher $\boldsymbol{f_1}$ means that it's difficult for human eyes to distinguish between text and background, i.e. lower quality score. The second feature $\boldsymbol{f_2}$ is designed for measuring blurness of text layer. Notably, we obtained the text layer $\boldsymbol{TL}$ ($\boldsymbol{TL}$=binary($TTL + STL$)) shown in Fig.3 by eliminating background pixels whose gray values are $\boldsymbol{B_d}$ from $\boldsymbol{M_t}$. We firstly adopted Matlab function $bwareaopen.m$ to eliminate

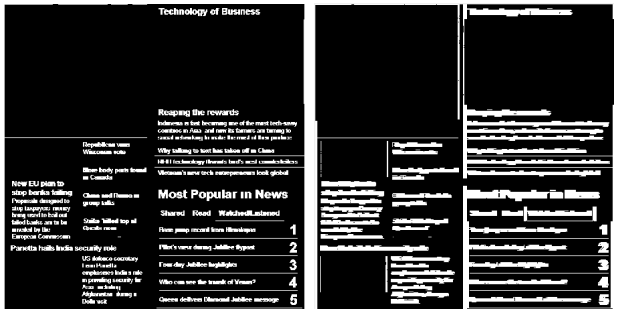

(a) (b)

Fig. 3. The text layer of (a) reference SCI ($N_{t,r}$=211), (b) distorted SCI corrupted by motion blur ($N_{t,d}$=34).

the tiny connected regions (noise) from $\boldsymbol{TL}$, then we utilized $bwconncomp.m$ to find out the number $\boldsymbol{N_{t,d}}$ of remaining connected regions of $\boldsymbol{TL}$. The $\boldsymbol{f_2}$ is calculated as

$$\boldsymbol{f_2} = \frac{|N_{t,r} - N_{t,d}|}{N_{t,r}} \tag{12}$$

where $\boldsymbol{N_{t,r}}$ is the number of connected regions of the reference SCI's text layer. Notably, we refined a brief vector $\boldsymbol{V_{r,t}}$=[$\boldsymbol{B_r}$, $\boldsymbol{N_{t,r}}$] containing only two parameters to represent text layer of the reference SCI. Heretofore, we obtained the quality score of text layer as $\boldsymbol{score_t} = \frac{1}{2}\boldsymbol{f_1} + \frac{1}{2}\boldsymbol{f_2}$. Eventually, the final quality score is defined as

$$\boldsymbol{score} = \theta \boldsymbol{score_p} + (1-\theta)\boldsymbol{score_t} \tag{13}$$

where the weighting coefficient θ is the area ration between pictorial layer and the whole SCI.

3. EXPERIMENTAL RESULT

We adopted SIQAD [3] as test database to validate the performance. SIQAD is a large-scale SCI quality assessment database consisting of 20 source and 980 distorted SCIs. The distortion types of SIQAD include Gaussian Noise (GN), Gaussian Blur (GB), Motion Blur (MB), Contrast Change (CC), JPEG, JPEG2000, and Layer Segmentation Based Coding (LSC). We compared the proposed method with state-of-the-art full-reference and reduced-reference quality metrics. Suggested by video quality experts group (VQEG) [14], we first used a logistic regression function $q(\boldsymbol{score}) = \beta_1(\frac{1}{2} - \frac{1}{1+exp(\beta_2(\boldsymbol{score}-\beta_3))}) + \beta_4\boldsymbol{score} + \beta_5$ to generate the mapped score, where $\beta_j (j = 1,2,3,4,5)$ are free parameters to be determined during the curve fitting process. Then we calculated the frequently used performance evaluations $PLCC$, $SROCC$ and $RMSE$ to validate the prediction accuracy.

The performances in SIQAD of competitive metrics have been reported in Table 1. Experimental results imply that the proposed method outperforms most general quality metrics, i.e. SSIM, VIF, VSI, PSNR, etc. Moreover, as a reduced-reference metric, the proposed method is highly competitive compared with full-reference metrics SPQA, SIQM, and Q_s dedicated for SCI. Notably, the performances shown in Table 2 indicate that we bold the top metric with Q_s in Gaussian Blur and Motion Blur distortions of SIQAD.

Table 1. Performance over all distortion types

IQA Metrics	PLCC	SROCC	RMSE
SSIM [4]	0.7445	0.7433	9.4713
PSNR	0.5788	0.5539	11.5691
VIF [15]	0.8026	0.7857	8.4642
VSI [16]	0.5403	0.5199	11.9384
FSIM [17]	0.5741	0.5647	11.6164
Q_s[5]	0.8573	0.8456	7.3030
SIQM [6]	0.8518	0.8452	7.4219
SPQA [3]	**0.8631**	**0.8579**	**7.2297**
Proposed	**0.8126**	**0.7962**	**8.2633**

Table 2. Performance over Gaussian Blur and Motion Blur

IQA Metrics	PLCC	SROCC	RMSE
SSIM [4]	0.8537	0.8481	7.1334
Q_s[5]	**0.8972**	**0.8856**	**6.7335**
SIQM [6]	0.8785	0.8750	6.9241
SPQA [3]	0.8687	0.8636	6.8262
Proposed	**0.8907**	**0.8846**	**6.7638**

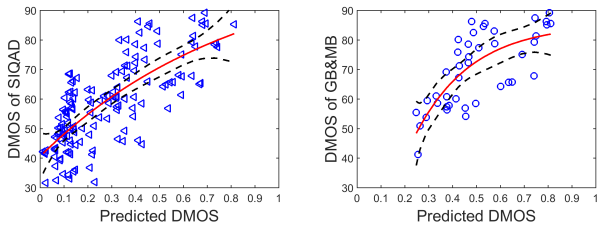

(a) (b)

Fig. 4. Scatter plots of the proposed metric over (a) all distortion types of SIQAD, (b) GB and MB distortions of SIQAD.

The scatter plots of DMOS versus the proposed metric on all distortion types and GB&MB distortions of SIQAD are presented in Fig.4, where the red lines are curves fitted with the logistic regression function and the blue dash lines are the 95% confidence intervals of the fitting.

4. CONCLUSION

In this paper, we firstly designed a novel layer-based segmentation method to divide SCI into text and pictorial layers. Subsequently, we proposed a reduced-reference SCI quality metric considering the perceptual characters of different regions. Validation experiments show encouraging performances, especially for blur distortions. The development of this metric for border application scenarios such as SCI corrupted by realistic distortions is worth addressing in the future.

5. REFERENCES

[1] H. Shen, Y. Lu, F. Wu, and S. Li, "A high-performanance remote computing platform," *in ICPCC*, pp. 1-6, Mar. 2009.

[2] C.-Y. Huang, C.-H. Hsu, Y.-C. Chang, and K.-T. Chen, "GamingAnywhere: An open cloud gaming system," *in ACM MSC*, pp. 36-47, 2013.

[3] Yang H, Fang Y, Lin W. "Perceptual quality assessment of screen content images." *IEEE Transactions on Image Processing*, 2015, 24(11): 4408-4421.

[4] Wang Z, Bovik A C, Sheikh H R, et al. "Image quality assessment: from error visibility to structural similarity." *Image Processing, IEEE Transactions on,* 2004, 13(4): 600-612.

[5] Wang S, Gu K, Zeng K, et al. "Perceptual screen content image quality assessment and compression," *IEEE International Conference on Image Processing. IEEE*, 2015:1434-1438.

[6] Gu K, Wang S, hai G, et al. "Screen image quality assessment incorporating structural degradation measurement," *IEEE International Symposium on Circuits and Systems. IEEE*, 2015:125-128.

[7] Shen C, Zhao Q. "Webpage saliency". *European Conference on Computer Vision, Springer International Publishing*, 2014: 33-46.

[8] Lin T, Hao P. "Compound image compression for real-time computer screen image transmission." *IEEE transactions on Image Processing*, 2005, 14(8): 993-1005.

[9] Pan Z, Shen H, Lu Y, et al. "A low-complexity screen compression scheme for interactive screen sharing." *Circuits and Systems for Video Technology, IEEE Transactions on*, 2013, 23(6): 949-960.

[10] Minaee S, Wang Y. "Screen content image segmentation using least absolute deviation fitting." *Image processing (ICIP)*, 2015 IEEE international conference on. IEEE, 2015: 3295-3299.

[11] Minaee S, Abdolrashidi A, Wang Y. "Screen content image segmentation using sparse-smooth decomposition." *2015 49th asilomar conference on signals, systems and computers*. IEEE, 2015: 1202-1206.

[12] Zhai G, Wu X, Yang X, et al. "A psychovisual quality metric in free-energy principle." *Image Processing, IEEE Transactions on,* 2012, 21(1): 41-52.

[13] He K, Sun J, Tang X, "Guided image filtering." *Pattern Analysis and Machine Intelligence, IEEE Transactions on*, 2013, 35(6): 1397-1409.

[14] Video Quality Experts Group et al., "Final report from the video quality experts group on the validation of objective models of video quality assessment," VQEG, Mar, 2000.

[15] Hamid R Sheikh and Alan C Bovik, "Image information and visual quality," *Image Processing, IEEE Transactions on*, vol. 15, no. 2, pp. 430C444, 2006.

[16] Lin Zhang, Lei Zhang, and Xuanqin Mou, "FSIM: a feature similarity index for image quality assessment," *Image Processing, IEEE Transactions on*, vol. 20, no. 8, pp. 2378C2386, 2011.

[17] Lin Zhang, Ying Shen, and Hongyu Li, "VSI: A visual saliency induced index for perceptual image quality assessment," *Image Processing, IEEE Transactions on,* vol. 23, no. 10, pp. 4270C4281, 2014.